Infrared Photodissociation Spectroscopy of Protonated Formic Acid and Acetic Acid Clusters

Yoshiya Inokuchi and Nobuyuki Nishi*

Institute for Molecular Science, Myodaiji, Okazaki 444-8585, Japan

Received: April 17, 2003; In Final Form: July 29, 2003

Infrared photodissociation spectra of protonated formic acid clusters, $H^+\cdot(HCOOH)_n$ ($n = 2-5$), are measured in the 3000−3700 cm^{-1} region. Density functional theory calculation is applied to $H^+\cdot(HCOOH)_n$ ($n = 2-5$). Geometry optimization of $H^+\cdot(HCOOH)_n$ ($n = 2-5$) indicates that stable forms of these clusters are open-chain structures with free OH groups at both ends. In the infrared photodissociation spectra of the $n = 2$ and $n = 3$ species, there are two sharp bands in the range of 3400−3700 cm^{-1}. The lower- and higher-frequency bands of them are attributed to the free OH stretching vibrations of the peripheral COOH groups in the E and Z conformations, respectively. The intensity of the higher-frequency band, relative to that of the lower-frequency band, decreases from $n = 2$ to $n = 3$. The $n = 4$ and $n = 5$ ions exhibit only one sharp band in the same region. This band is assigned to the free OH stretching vibrations of the end COOH groups in the E conformation; the $n = 4$ and $n = 5$ ions have the peripheral COOH groups only in the E conformation. We observe infrared photodissociation spectra of $H^+\cdot(HCOOH)_n$ ($n = 6, 7$) in the 3500−3600 cm^{-1} region. The absence of any free OH band for $n = 7$ shows that both ends of chain structures of $n = 7$ are terminated by cyclic dimers. Infrared photodissociation spectra of $H^+\cdot(CH_3COOH)_n$ ($n = 2-5$) are also examined in the 3000−3700 cm^{-1} region. Resemblance of the spectra of $H^+\cdot(CH_3COOH)_n$ to those of $H^+\cdot(HCOOH)_n$ suggests that the acetic acid clusters have structures that are similar to those of the formic acid clusters; the intermolecular network is formed only by the COOH groups.

1. Introduction

Carboxylic acid (RCOOH) is one of the popular acids in organic chemistry. Much research have been devoted to elucidating the intermolecular configurations between carboxylic acid molecules.[1−11] In crystals, carboxylic acid molecules are interlinked to form either a cyclic dimer or an infinite chain; the manner of linkage depends on the substituent R.[1] Formic acid forms an infinite chain in the crystal[1] and a cyclic dimer in the gas phase.[11] Lifshitz and co-workers have extensively investigated protonated carboxylic acid clusters.[12−15] They generated the clusters using electron-impact ionization and observed the unimolecular dissociation.[12,13] The $H^+\cdot(RCOOH)_n$ clusters with $n \leq 5$ mainly release a neutral monomer. A neutral dimer also evaporates from the clusters that are larger than $n = 5$. They also performed ab initio calculation of the clusters.[14] The structures optimized by the calculation corroborated the manner of dissociation. Open-chain structures with one or two free OH group(s) at the periphery are favored energetically for $n \leq 5$. Chain structures terminated by cyclic dimer units are preferable for $n \geq 6$.

Vibrational spectroscopy is one of the most powerful methods for the structural investigation of molecules and clusters. In particular, infrared photodissociation spectroscopy is quite useful for the study of molecular cluster ions.[16−20] We have applied this spectroscopy to the protonated formic acid−water binary clusters, $H^+\cdot(HCOOH)_n\cdot H_2O$ ($n = 1-5$).[21] From the infrared photodissociation spectra of the clusters, we can conclude that the clusters switch the ion cores from $HCOOH_2^+$ ($H^+\cdot(HCOOH)_n\cdot H_2O$, $n = 1-3$) to H_3O^+ ($H^+\cdot(HCOOH)_n\cdot H_2O$, $n = 4, 5$). The $H^+\cdot(HCOOH)_5\cdot H_2O$ ion has the cyclic-type structure; the H_3O^+ ion core is fully surrounded and stabilized by five HCOOH molecules.

In this paper, we report structural studies on $H^+\cdot(HCOOH)_n$ and $H^+\cdot(CH_3COOH)_n$ ($n = 2-5$). Infrared photodissociation spectra of the clusters are measured in the 3000−3700 cm^{-1} region. For the formic acid system, we extend the measurement size up to $n = 7$. Geometries are optimized and vibrational frequencies are evaluated by density functional theory (DFT) calculation for $H^+\cdot(HCOOH)_n$ ($n = 2-5$). In this paper, the conformation of the COOH group is designated as Z when the H atom of the OH group and the substituent R are situated on the same side of the C−O single bond, whereas the designation E is used for the conformation in which the R substituent and the H atom are on opposite sides. We discuss the stability of the E and Z conformations in the peripheral COOH groups of open-chain structures on the basis of the infrared photodissociation spectra and the results of geometry optimization.

2. Experimental and Computational Section

The infrared photodissociation spectra of $H^+\cdot(HCOOH)_n$ and $H^+\cdot(CH_3COOH)_n$ are measured by an ion-guide spectrometer with two quadrupole mass filters.[22] Figure 1 displays a schematic diagram of the spectrometer. The spectrometer is differentially pumped by three oil-diffusion pumps and one turbo molecular pump, and the pressure at the photodissociation area is $\sim 5 \times 10^{-6}$ Pa during operation of a pulsed nozzle. A gas mixture of carboxylic acid (~3% content) and argon is introduced into the vacuum chamber through the pulsed nozzle (General Valve Series 9) with an orifice diameter of 0.80 mm, a pulse duration of 300 μs, and a repetition rate of 10 Hz. The total stagnation

* Author to whom correspondence should be addressed. E-mail: nishi@ims.ac.jp.

10.1021/jp030475n CCC: $25.00
Published on Web 11/26/2003

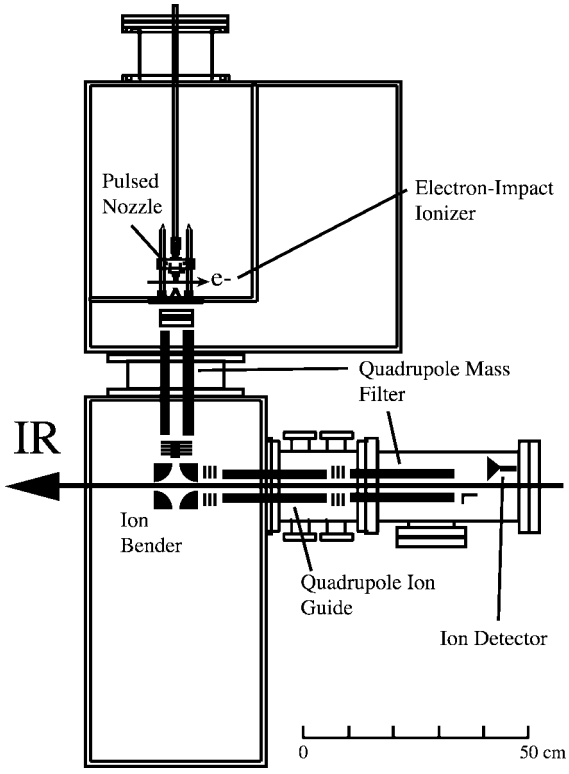

Figure 1. Schematic diagram of the photodissociation spectrometer.

pressure is 1×10^5 Pa. Neutral clusters are ionized by a homemade electron-impact ionizer that is situated near the exit of the pulsed nozzle. The electron kinetic energy is adjusted to 350 eV. After passing through a skimmer, cluster ions are accelerated into the spectrometer with a 50 eV kinetic energy by a high-voltage pulse switch (Matsusada model HSK-1P20-00). Parent ions are isolated by the first quadrupole mass filter. The number of isolated parent ions is on the order of 100 per pulse. After deflection by 90° through an ion bender, parent ions are led into a quadrupole ion guide. The ion beam is merged with an infrared laser beam in the ion guide, and the parent ions are promoted to vibrationally excited states. The excitation induces fragmentation of the parent ions; up to ~10% of parent ions are dissociated by the infrared laser. Resultant fragment ions are mass-analyzed by the second quadrupole mass filter and detected by a secondary electron multiplier tube. For normalization of the fragment-ion yield, the power of the dissociation laser is monitored by a pyroelectric detector (Molectron model P1-15H-CC) after the laser beam passes through the spectrometer. Both ion signals from the ion detector and laser signals from the pyroelectric detector are fed into a digital storage oscilloscope (LeCroy model 9314A) and averaged over 200 shots for one point of a spectrum. The oscilloscope is controlled by a microcomputer through a general purpose interface bus (GPIB). Infrared photodissociation spectra of parent ions are obtained by plotting the normalized yields of fragment ions against wavenumber of the dissociation laser. One carboxylic acid molecule evaporates from the clusters after the irradiation of the infrared laser; no other fragmentation can be observed in our experiment.

The tunable infrared source used in this study is an optical parametric oscillator (OPO) system (Continuum Mirage 3000) that is pumped with an injection-seeded Nd:YAG laser (Continuum Powerlite 9010). The output energy is 1−2 mJ per pulse, and the line width is ~1 cm^{-1}; we use the OPO laser with the broad band mode by blocking the pump beam for the first oscillator stage. The infrared laser is loosely focused by a CaF_2 lens (a focal length of 1000 mm) located just before the spectrometer. The wavenumber of the OPO laser is calibrated by a commercial wavemeter (Burleigh model WA-4500).

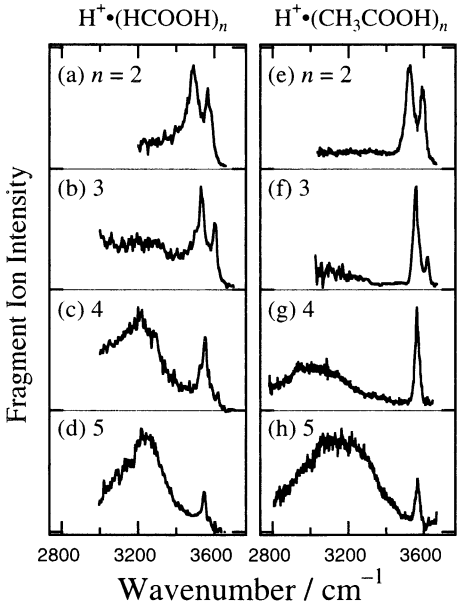

Figure 2. (a−d) Infrared photodissociation spectra of $H^+\cdot(HCOOH)_n$ and (e−h) $H^+\cdot(CH_3COOH)_n$, with $n = 2-5$, in the 3000−3700 cm^{-1} region.

TABLE 1. Observed Band Positions, Calculated Band Positions and Intensities, and Assignments of the Free OH Stretching Vibrations of $H^+\cdot(RCOOH)_n$ (R = H and CH_3)

R = H (cm^{-1})	calculated (R = H) band position (cm^{-1})[a]	R = CH_3 (cm^{-1})	assignment
	$n = 2$		
3489	3505 (331),[b] 3506 (0)[b]	3524	E-type COOH
	3499 (174)[c]		E-type COOH
3565	3572 (211)[c]	3590	Z-type COOH
	$n = 3$		
3532	3527 (119),[b] 3549 (97)[b]	3557	E-type COOH
	3529 (115)[c]		E-type COOH
3600	3585 (168)[c]	3617	Z-type COOH
	$n = 4$		
3547	3534 (107),[b] 3550 (86)[b]	3564	E-type COOH
	$n = 5$		
3545	3541 (93),[b] 3552 (82)[b]	3566	E-type COOH

[a] A scaling factor of 0.9521 was used. Values given in parentheses are intensities, given in units of km/mol. [b] Value of (E, E) isomer. [c] Value of (E, Z) isomer.

Moreover, the $H^+\cdot(HCOOH)_n$ ($n = 2-5$) clusters are analyzed by DFT calculation. The calculation is made with the Gaussian 98 program package.[23] Geometry optimization and vibrational frequency evaluation are conducted at the B3LYP/6-31++G(d,p) level of theory. Calculation at this level has been successful for the protonated formic acid−water binary clusters.[21]

3. Results and Discussion

3.1. Infrared Photodissociation Spectra and Optimized Structures of $H^+\cdot(HCOOH)_n$ ($n = 2-5$). Figure 2 displays the infrared photodissociation spectra of $H^+\cdot(HCOOH)_n$ with $n = 2-5$ (spectra a−d). Two sharp bands are present, at 3489 and 3565 cm^{-1} for $n = 2$ and at 3532 and 3600 cm^{-1} for $n = 3$. For the $n = 4$ and $n = 5$ ions, only one sharp band emerges, at 3547 and 3545 cm^{-1}, respectively. Table 1 collects the band

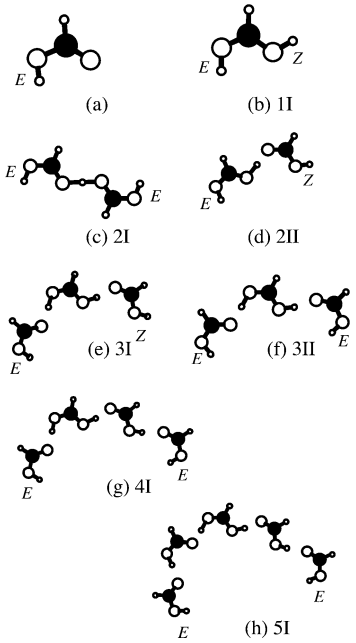

Figure 3. Optimized structures of (a) HCOOH and $H^+\cdot(HCOOH)_n$ with (b) $n = 1$, (c, d) $n = 2$, (e, f) $n = 3$, (g) $n = 4$, and (h) $n = 5$.

positions. The sharp bands in the 3400−3700 cm^{-1} region can be assigned to the free OH stretching vibration of the COOH group. The $n = 3$ spectrum shows a broad hump at ∼3200 cm^{-1}. The $n = 4$ and $n = 5$ ions have a broad band with a maximum at ∼3230 cm^{-1}.

Structures of HCOOH and $H^+\cdot(HCOOH)_n$ ($n = 1-5$) that have been optimized by DFT calculations are shown in Figure 3. Previously, ab initio molecular orbital calculations of these species were performed by Zhang and Lifshitz.[14] They mentioned that open-chain structures with free OH groups at the ends are favored energetically for $H^+\cdot(HCOOH)_n$ with $n \leq 5$. We can see the same trend in our calculations; the most-stable and second-most-stable structures have open-chain forms for $n = 2-5$. The neutral HCOOH molecule has the E conformation (Figure 3a).[24] In the most-stable structure of the $n = 1$ ion, both the E and Z conformations coexist (isomer 1I, Figure 3b). The most-stable and second-most-stable structures of $n = 2$ (isomers 2I and 2II) are displayed in Figure 3c and 3d. In isomer 2I, a proton is equally shared by the two molecules with the E-type COOH. This structure was not obtained in the previous study.[14] Isomer 2II has an $HCOOH_2^+$ ion core. The COOH group of the solvent molecule bound to the ion core shows the *Z* conformation. In the most-stable structure of $n = 3$, the peripheral COOH groups are in the E and Z conformations (isomer 3I, Figure 3e). The second-most-stable form has the E-type COOH groups at both ends (isomer 3II, Figure 3f). In contrast, the conformations of the end COOH groups are E-type in the most-stable structures of the $n = 4$ and $n = 5$ ions, as shown in Figure 3g and 3h (isomers 4I and 5I). We have tabulated the calculated absolute energies, energies relative to the most-stable isomers, binding energies, and combinations of the peripheral COOH conformations in Table 2. Hereafter, we call the open-chain cluster with the peripheral COOH groups in the E and Z conformations an (E, Z) isomer. Other structures such as (Z, Z) isomers or non-open-chain isomers are less stable than the most-stable isomers with $\Delta E > 800$ cm^{-1}. The ΔE values of $n = 2-5$ shown in Table 2 are small; therefore, it is impossible to assign structures of the observed clusters only from the optimized structures. We determine the cluster structures from the comparison of the observed infrared spectra with calculated spectra. The calculated binding energies exceed the energy of the infrared laser used in this study (3000−3700 cm^{-1}). Multiphoton processes are necessary for the dissociation of cold clusters. In our spectrometer, however, multiphoton processes rarely occur, because of the sparse photon density in the ion guide.[22] Therefore, the cluster ions are dissociated through the one-photon absorption, with the assistance of internal energies.

TABLE 2. DFT-Calculated Absolute Energies (E_{ZPVE}), Energies Relative to the Most Stable Isomers (ΔE), Binding Energies (E_{bind}), and Combinations of Peripheral COOH Conformations of Chain Structures for $H^+\cdot(HCOOH)_n$ ($n = 1-5$)

n	isomer	E_{ZPVE}[a] (hartree)	ΔE (cm^{-1})	E_{bind}[c] (cm^{-1})	combination
	HCOOH	−189.741817			
1	1I	−190.021302			(*E*, *Z*)
2	2I	−379.813789	0	11121	(*E*, *E*)
	2II	−379.811395	+525	10595	(*E*, *Z*)
3	3I	−569.583470	0	6115	(*E*, *Z*)
	3II	−569.582312	+254	5861	(*E*, *E*)
4	4I	−759.348576	0	5111	(*E*, *E*)
	4II[b]	−759.348328	+54	5057	(*E*, *Z*)
5	5I	−949.110767	0	4472	(*E*, *E*)
	5II[b]	−949.109117	+362	4109	(*E*, *Z*)

[a] Corrected with zero-point vibrational energies. [b] These isomers are not shown in Figure 3. [c] $E_{bind}(n) = -E_{ZPVE}(n) + E_{ZPVE}(n-1) + E_{ZPVE}(HCOOH)$, where $E_{ZPVE}(n-1)$ is the energy of the most-stable isomer of the $(n-1)$ ion.

3.2. $H^+\cdot(HCOOH)_2$. The isomers of $n = 2$ have two bands of the free OH stretching vibrations in the 3400−3600 cm^{-1} region. For isomer 2I, asymmetric and symmetric stretching vibrations of the free OH groups are calculated to be 3505 and 3506 cm^{-1}, respectively. For isomer 2II, the free OH oscillator of the $HCOOH_2^+$ ion core has a frequency of 3499 cm^{-1}. The free OH stretching frequency of the solvent HCOOH is 3572 cm^{-1}. The vibrational frequencies of the optimized structures are listed in Table 1. The free OH bands of the COOH groups in the E conformation show the frequencies almost the same as each other (3505, 3506, and 3499 cm^{-1}). The COOH group in the *Z* conformation has a free OH stretching frequency (3572 cm^{-1}) that is higher than those in the E conformation by ∼70 cm^{-1}. In the observed spectrum of $n = 2$, two bands emerge at 3489 and 3565 cm^{-1}. The frequency difference between the two bands is 76 cm^{-1}, which is almost coincident with the calculated frequency difference (∼70 cm^{-1}). Therefore, we assign the bands observed at 3489 and 3565 cm^{-1} to the free OH stretching vibrations of the peripheral COOH groups in the E and Z conformations, respectively. Although the most-stable isomer is the (E, E) isomer (isomer 2I), the appearance of the band of the Z conformation suggests the presence of the (E, Z) isomer (isomer 2II) in our experiment. On the basis of the band intensities observed and calculated, we can estimate the abundance of the (E, E) isomer, relative to the (E, Z) isomer. In the observed spectrum, the intensity of the 3565 cm^{-1} band, relative to the 3489 cm^{-1} band, is 0.45. For the (E, Z) isomer (isomer 2II), the infrared intensities of the free OH oscillators on the E and Z sites are 174 and 211 km/mol, whereas the free OH stretching vibrations of the (E, E) isomer (isomer 2I) has intensities of 331 and 0 km/mol. If the two isomers equally contribute to the infrared spectrum, the intensity of the free OH band of the Z-type COOH group, relative to that of the E-type groups, is $211/(174 + 331 + 0) = 0.42$. This value is very similar to the observed relative intensity (0.45). Therefore, the (E, Z) and (E, E) isomers are equally present for $n = 2$ in our experiment.

3.3. H^+·(HCOOH)$_3$. For $n = 3$, the infrared photodissociation spectrum shows two bands, at 3532 and 3600 cm^{-1}. The most-stable isomer (isomer 3I) has the free OH stretching vibrations at 3529 and 3585 cm^{-1}. Because the calculated band positions are close to the observed positions, we can ascribe the 3532 and 3600 cm^{-1} bands to the free OH stretching vibrations of the E- and Z-type COOH groups of isomer 3I, respectively. However, there is a discrepancy in the intensity of the two bands between the observed and calculated spectra. In the observed spectrum, the intensity of the 3600 cm^{-1} band, relative to that of the 3532 cm^{-1} band, is 0.25. The infrared intensities of the free OH stretching vibrations of the E- and Z-type COOH groups are calculated to be 115 and 168 km/mol for isomer 3I; the relative intensity is 1.5. The introduction of isomer 3II (Figure 3f) resolves the discrepancy. For isomer 3II, the free OH stretching vibrations of the peripheral E-type COOH groups exhibit intensities of 119 and 97 km/mol. From the infrared intensities calculated for isomers 3I and 3II, the intensity of the free OH oscillators of the Z-type COOH group, relative to that of the E-type COOH groups, is $168/(115 + 119x + 97x)$, where x represents the abundance of isomer 3II, relative to that of isomer 3I. From the observed relative intensity of 0.25, we obtain $x = 2.6$. The (E, E) isomer (isomer 3II) is 2.6 times more abundant than the (E, Z) isomer (isomer 3I), although the (E, E) isomer is less stable than the (E, Z) isomer, by 254 cm^{-1}.

3.4. H^+·(HCOOH)$_n$ (n = 4, 5). Each of the infrared photodissociation spectra of $n = 4$ and $n = 5$ shows only one sharp band, at 3547 and 3545 cm^{-1}, respectively. Calculated frequencies of the free OH stretching vibrations of the (E, E) isomers are 3534 and 3550 cm^{-1} for $n = 4$, and 3541 and 3552 cm^{-1} for $n = 5$; the average values are 3542 and 3547 cm^{-1} for $n = 4$ and $n = 5$, respectively. These values coincide well with the observed band positions. Therefore, the bands observed at 3547 and 3545 cm^{-1} for $n = 4$ and $n = 5$ are assigned to the free OH stretching vibrations of the peripheral E-type COOH groups. No band due to the Z conformation is observed, which suggests that the $n = 4$ and $n = 5$ ions have only the (E, E) isomers (isomers 4I and 5I). The abundance of the (E, E) isomer, relative to that of the (E, Z) isomer, increases as the cluster size increases from $n = 2$ to $n = 5$, which suggests that the (E, E) isomer is preferable for larger clusters.

3.5. Charge Effect on Infrared Band Positions and Termination of Chain Structures. The observed frequencies of the free OH oscillators of the E-type COOH groups increase as the cluster size increases (3489, 3532, 3547, and 3545 cm^{-1} for $n = 2$, $n = 3$, $n = 4$, and $n = 5$, respectively). The values of the $n = 4$ and $n = 5$ ions are similar to that of neutral formic acid in the E conformation (3550.5 cm^{-1}).[24] The frequency calculations of H^+·(HCOOH)$_n$ exhibit a similar trend; the average frequencies of the free OH oscillators in the E-type COOH groups are 3503, 3535, 3542, and 3547 cm^{-1} for $n = 2$, $n = 3$, $n = 4$, and $n = 5$, respectively. The increase in the frequency is related to the decrease in the charge on the end molecules. From the Mulliken charge, we can obtain the charge on the peripheral HCOOH molecules. For isomer 2I, the proton is equally shared by the two molecules in the E conformation; the charge on the HCOOH molecules is thought to be 0.50. In isomer 2II, the E-type COOH group is in the $HCOOH_2^+$ ion core; the charge on the ion core is 0.87. Therefore, the average charge on the molecules with E-type COOH groups is $(0.5 + 0.5 + 0.87)/3 = 0.62$ for $n = 2$. The average charges on the peripheral E-type HCOOH molecules are calculated to be 0.084, 0.054, and 0.039 for the $n = 3$, $n = 4$, and $n = 5$ ions, respectively.

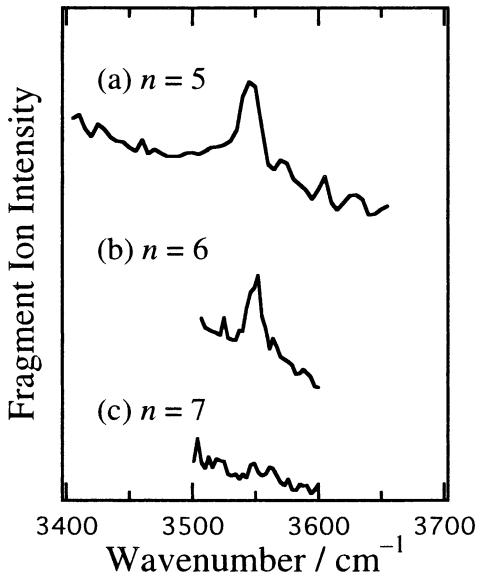

Figure 4. Infrared photodissociation spectra of H^+·(HCOOH)$_n$, with $n = 5-7$, in the free OH stretching region.

The decrease in the charge on the end molecules also changes the relative stability between the E and Z conformations in the peripheral COOH groups. The most-stable isomer of the $n = 1$ ion is the (E, Z) isomer. For $n = 2$ and $n = 3$, both the (E, Z) and (E, E) isomers are present in our experiment; the abundance of the (E, E) isomer, relative to that of the (E, Z) isomer, increases from $n = 2$ to $n = 3$. In the case of $n = 4$ and $n = 5$, the (E, E) isomer is the dominant species. In the previous study, it was shown that chain structures that have been terminated by cyclic dimer units at both ends become preferable for larger clusters (see Figures 4, 5, and 8 of ref 14). For the formation of a cyclic dimer, both of the constituent HCOOH molecules should have the E conformation. The structure of isomer 5I indicates that the $n = 5$ ion can probably get another HCOOH molecule and form a cyclic dimer at one end of the chain. Figure 4 displays the infrared photodissociation spectra of H^+·(HCOOH)$_n$ ($n = 5-7$) in the free OH region. A sharp band can be observed at 3552 cm^{-1} for $n = 6$. This band is assigned to the free OH stretching vibration of the E-type COOH group; there is at least one free OH group at the periphery. In contrast, one cannot see any band in the spectrum of $n = 7$, implying that both ends of chain structures are completely terminated by cyclic dimers for $n = 7$. The $n = 6$ ion may be terminated by a cyclic dimer unit at one end. The probable structures of the $n = 6$ and $n = 7$ clusters are well coincident with the structures predicted from the results of the unimolecular dissociation; a neutral dimer evaporates from the clusters that are larger than $n = 5$.[12,13]

3.6. Assignment of Infrared Photodissociation Spectra of H^+·(HCOOH)$_n$ ($n = 3-5$) in the 3000−3400 cm^{-1} Region. In the infrared photodissociation spectrum of the $n = 3$ ion, a broad band is observed in the 3000−3700 cm^{-1} region; the intensity increases as the frequency decreases. We assign this absorption to the hydrogen-bonded OH stretching vibrations of the $HCOOH_2^+$ ion core, although the maxima may be located at lower than 3000 cm^{-1}. The calculations predict the hydrogen-bonded OH bands at 2169 and 2425 cm^{-1} for isomer 3I, and 2044 and 2683 cm^{-1} for isomer 3II. The $n = 4$ and $n = 5$ ions show one broad band, with a maximum at 3220 and 3240 cm^{-1}, respectively. These bands are ascribed to the hydrogen-bonded OH stretching vibrations of the HCOOH molecules that are directly bound to the $HCOOH_2^+$ ion core. Calculated frequencies

are 3100 cm^{-1} for isomer 4I, and 2818 and 3183 cm^{-1} for isomer 5I. Apparently, the agreement of the observed frequencies with the calculated frequencies is not so good for the hydrogen-bonded OH oscillators. It is also the case for $H^+ \cdot (HCOOH)_n \cdot H_2O$ ($n = 4, 5$); calculations are prone to predict frequencies that are lower than those observed for the hydrogen-bonded OH oscillators, although the agreement is comparatively good for the free OH oscillators.[21]

3.7. $H^+ \cdot (CH_3COOH)_n$ ($n = 2-5$). The infrared photodissociation spectra of $H^+ \cdot (CH_3COOH)_n$ ($n = 2-5$) are shown in Figure 2e−h. The spectra resemble those of the formic acid clusters well (see Figure 2a−d). Two sharp bands are observed, at 3524 and 3590 cm^{-1} for $n = 2$, and at 3557 and 3617 cm^{-1} for $n = 3$. The intensity of the higher-frequency band, relative to that of the lower-frequency band, decreases from $n = 2$ to $n = 3$. On the basis of the band assignment of the formic acid clusters, the lower- and higher-frequency bands of $n = 2$ and $n = 3$ are attributed to the free OH stretching vibrations of the COOH groups in the E and Z conformations, respectively. The $n = 4$ and $n = 5$ ions display only one sharp band, at 3564 and 3566 cm^{-1}, respectively. These bands of $n = 4$ and $n = 5$ are assigned to the free OH stretching vibrations of the E-type COOH groups. Resemblance of the acetic acid spectra to the formic acid ones manifests similar intermolecular configurations; the intermolecular network is formed only by the COOH groups. This experimental result is consistent with the theoretical findings reported by Zhang and Lifshitz.[14] They suggested that the stable structures of the acetic acid clusters could be deduced by replacing the H atom by a CH_3 molecule in the optimized structures of the formic acid clusters. In detail, the respective band positions of the acetic acid clusters are slightly different from those of the formic acid clusters. Table 1 shows that the band positions of the acetic acid clusters are higher than those of the formic acid clusters, by ~20 cm^{-1}. This phenomenon is attributed to the frequency increase in the OH stretching vibration (3577 cm^{-1} for acetic acid)[25] from that of formic acid (3550.5 cm^{-1}).[24]

4. Conclusion

The infrared photodissociation spectra of $H^+ \cdot (HCOOH)_n$ and $H^+ \cdot (CH_3COOH)_n$ ($n = 2-5$) have been measured in the 3000−3700 cm^{-1} region. For $H^+ \cdot (HCOOH)_n$, the intensity of the free OH stretching band of the *Z*-type COOH group decreases as the cluster size increases from $n = 2$ to $n = 3$. The $n = 4$ and $n = 5$ ions have only the (E, E) isomers. These results show that the (E, E) isomer becomes more stable than the (E, Z) isomer for larger clusters. The infrared photodissociation spectrum of $H^+ \cdot (HCOOH)_7$ implies that both ends of chain structures are terminated by cyclic dimers. The infrared photodissociation spectra of the acetic acid clusters are quite similar to those of the formic acid clusters, which indicates that the acetic acid clusters have structures that are almost the same as those of the formic acid clusters. The intermolecular network is formed only by the COOH groups.

References and Notes

(1) Leiserowitz, L. *Acta Crystallogr., Sect. B: Struct. Crystallogr. Cryst. Chem.* **1976**, *B32*, 775.
(2) Cook, K. D.; Taylor, J. W. *Int. J. Mass Spectrom. Ion Phys.* **1980**, *35*, 259.
(3) Mori, Y.; Kitagawa, T. *Int. J. Mass Spectrom. Ion Processes* **1985**, *64*, 169.
(4) Mori, Y.; Kitagawa, T. *Int. J. Mass Spectrom. Ion Processes* **1988**, *84*, 305.
(5) Mori, Y.; Kitagawa, T. *Int. J. Mass Spectrom. Ion Processes* **1988**, *84*, 330.
(6) Sievert, R.; Cadez, I.; Van Doren, J.; Castleman, Jr., A. W. *J. Phys. Chem.* **1984**, *88*, 4502.
(7) Keesee, R. G.; Sievert, R.; Castleman, Jr., A. W. *Ber. Bunsen−Ges. Phys. Chem.* **1984**, *88*, 273.
(8) Meot-Ner, M. *J. Am. Chem. Soc.* **1992**, *114*, 3312.
(9) Tsuchiya, M.; Teshima, S.; Shigihara, A.; Hirano, T. *J. Mass Spectrom. Soc. Jpn.* **1998**, *46*, 483.
(10) Nishi, N.; Nakabayashi, T.; Kosugi, K. *J. Phys. Chem. A* **1999**, *103*, 10851.
(11) Karle, J.; Brockway, L. O. *J. Am. Chem. Soc.* **1944**, *66*, 574.
(12) Feng, W. Y.; Lifshitz, C. *J. Phys. Chem.* **1994**, *98*, 6075.
(13) Lifshitz, C.; Feng, W. Y. *Int. J. Mass Spectrom. Ion Processes* **1995**, *146/147*, 223.
(14) Zhang, R.; Lifshitz, C. *J. Phys. Chem.* **1996**, *100*, 960.
(15) Aviyente, V.; Zhang, R.; Varnali, T.; Lifshitz, C. *Int. J. Mass Spectrom. Ion Processes* **1997**, *161*, 123.
(16) Yeh, L. I.; Okumura, M.; Myers, J. D.; Price, J. M.; Lee, Y. T. *J. Chem. Phys.* **1989**, *91*, 7319.
(17) Bieske, E. J.; Maier, J. P. *Chem. Rev.* **1993**, *93*, 2603.
(18) Lisy, J. M. *Cluster Ions*; Wiley: Chichester, U.K., 1993; p 217.
(19) Ohashi, K.; Izutsu, H.; Inokuchi, Y.; Hino, K.; Nishi, N.; Sekiya, H. *Chem. Phys. Lett.* **2000**, *321*, 406.
(20) Ohashi, K.; Inokuchi, Y.; Izutsu, H.; Hino, K.; Yamamoto, N.; Nishi, N.; Sekiya, H. *Chem. Phys. Lett*. **2000**, *323*, 43.
(21) Inokuchi, Y.; Nishi, N. *J. Phys. Chem. A* **2002**, *106*, 4529.
(22) Inokuchi, Y.; Nishi, N. *J. Chem. Phys.* **2001**, *114*, 7059.
(23) Frisch, M. J.; Trucks, G. W.; Schlegel, H. B.; Scuseria, G. E.; Robb, M. A.; Cheeseman, J. R.; Zakrzewski, V. G.; Montgomery, J. A., Jr.; Stratmann, R. E.; Burant, J. C.; Dapprich, S.; Millam, J. M.; Daniels, A. D.; Kudin, K. N.; Strain, M. C.; Farkas, O.; Tomasi, J.; Barone, V.; Cossi, M.; Cammi, R.; Mennucci, B.; Pomelli, C.; Adamo, C.; Clifford, S.; Ochterski, J.; Petersson, G. A.; Ayala, P. Y.; Cui, Q.; Morokuma, K.; Malick, D. K.; Rabuck, A. D.; Raghavachari, K.; Foresman, J. B.; Cioslowski, J.; Ortiz, J. V.; Stefanov, B. B.; Liu, G.; Liashenko, A.; Piskorz, P.; Komaromi, I.; Gomperts, R.; Martin, R. L.; Fox, D. J.; Keith, T.; Al-Laham, M. A.; Peng, C. Y.; Nanayakkara, A.; Gonzalez, C.; Challacombe, M.; Gill, P. M. W.; Johnson, B. G.; Chen, W.; Wong, M. W.; Andres, J. L.; Head-Gordon, M.; Replogle, E. S.; Pople, J. A. *Gaussian 98*, revision A.9; Gaussian, Inc.: Pittsburgh, PA, 1998.
(24) Pettersson, M.; Lundell, J.; Khriachtchev, L.; Räsänen, M. *J. Am. Chem. Soc.* **1997**, *119*, 11715.
(25) Wilmshurst, J. K. *J. Chem. Phys.* **1956**, *25*, 1171.